Supplementary Materials

Oxygen coordinated Cu single atom catalysts: a superior catalyst towards electrochemical CO_2 reduction for methane production

Jundi Qin[#], Xiao Hu[#], Kanghua Miao, Xiongwu Kang

School of Environment and Energy, South China University of Technology, Guangzhou 510006, Guangdong, China.

[#]Authors contributed equally.

Correspondence to: Prof. Xiongwu Kang, School of Environment and Energy, South China University of Technology, 382 East Waihuan Road, Higher Education Mega Center, Guangzhou, China, 510006. Email: esxkang@scut.edu.cn

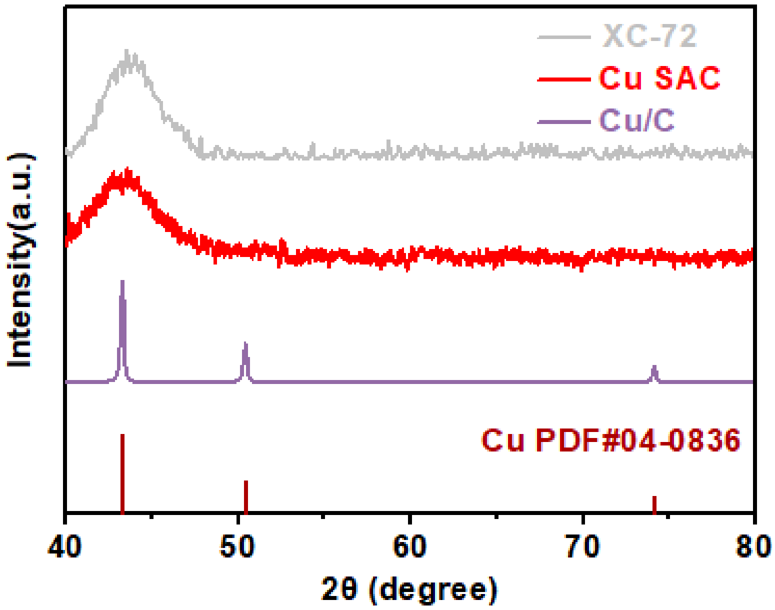

Figure S1. XRD patterns of Cu/C and Cu SAC.

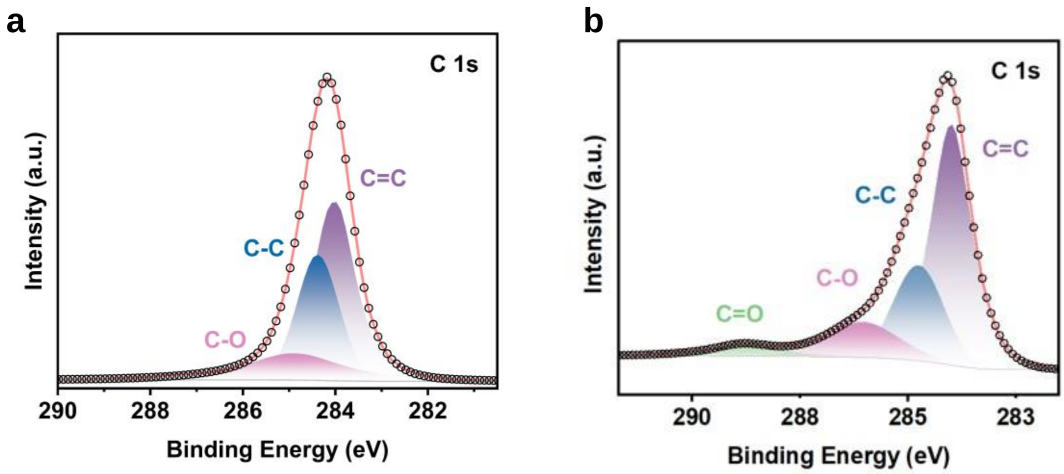

Figure S2. XPS of C 1s for (a) Cu/C and (b) Cu SAC.

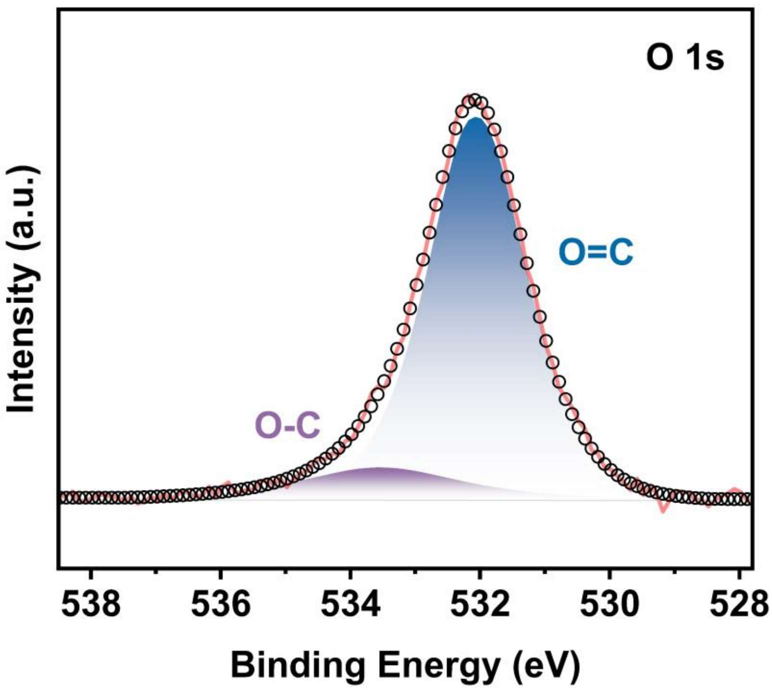

Figure S3. XPS of O 1s of Cu/C.

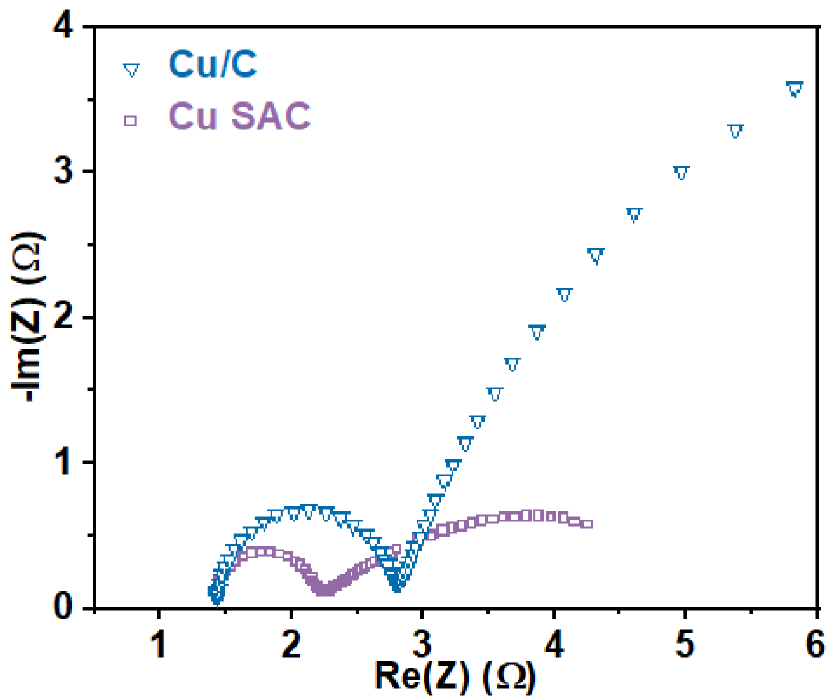

Figure S4. Nyquist plots in the frequency range 1 M Hz to 0.01Hz at –1.0V vs. RHE.

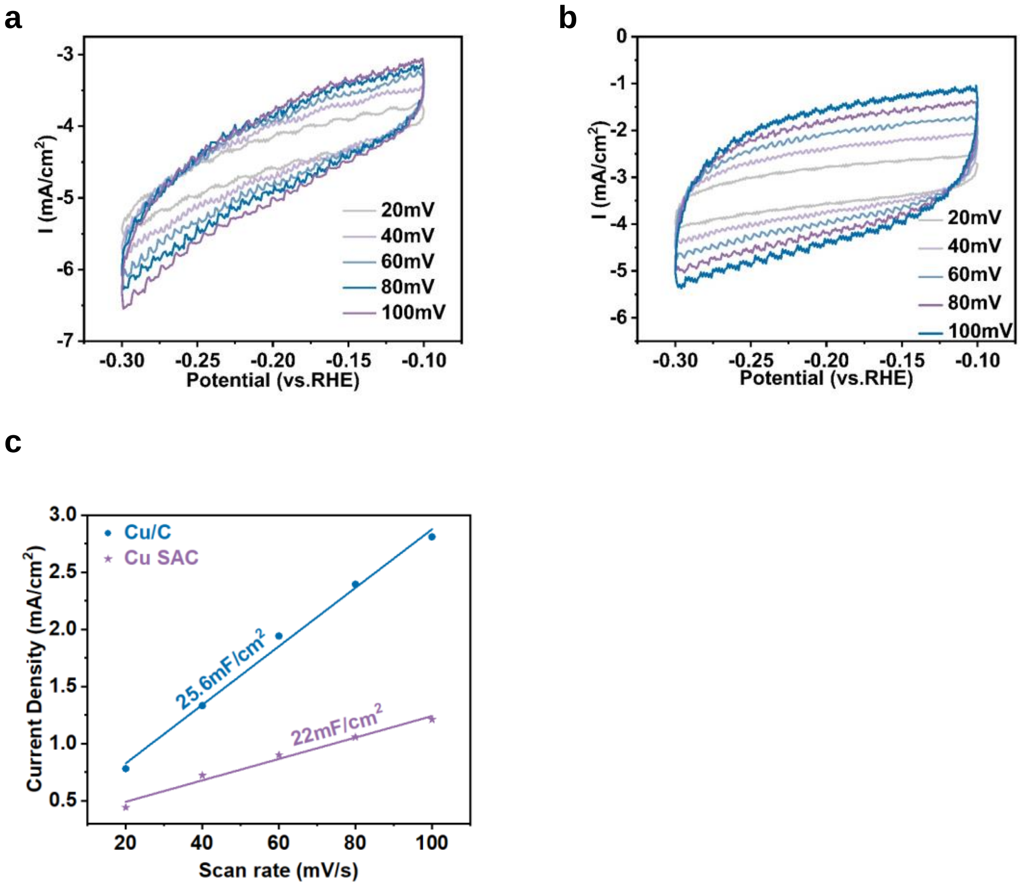

Figure S5. Double-layer capacitance of (a) Cu SAC and (b) Cu/C at different scan rate. (c) Electrochemically surface areas estimated from the double-layer capacitance of the samples.

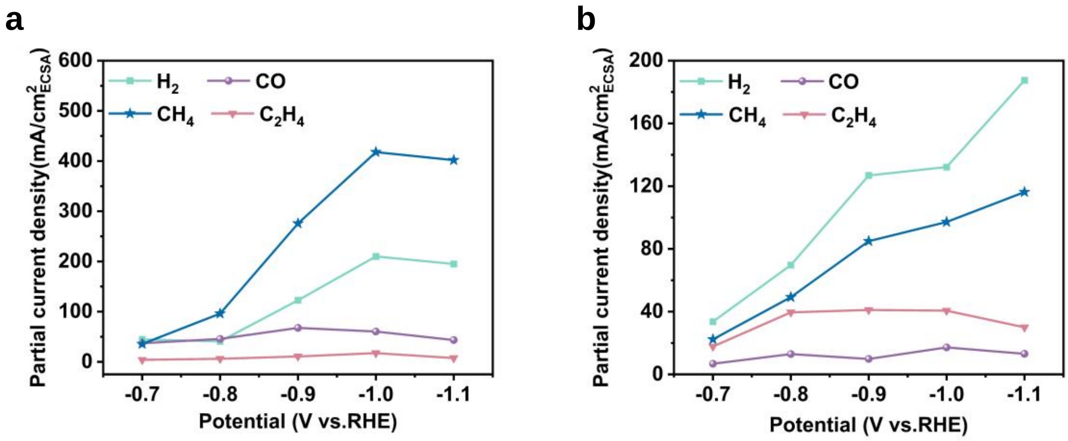

Figure S6. Partial current density of each product normalized to the ECSA: (a) Cu SAC; (b) Cu/C.

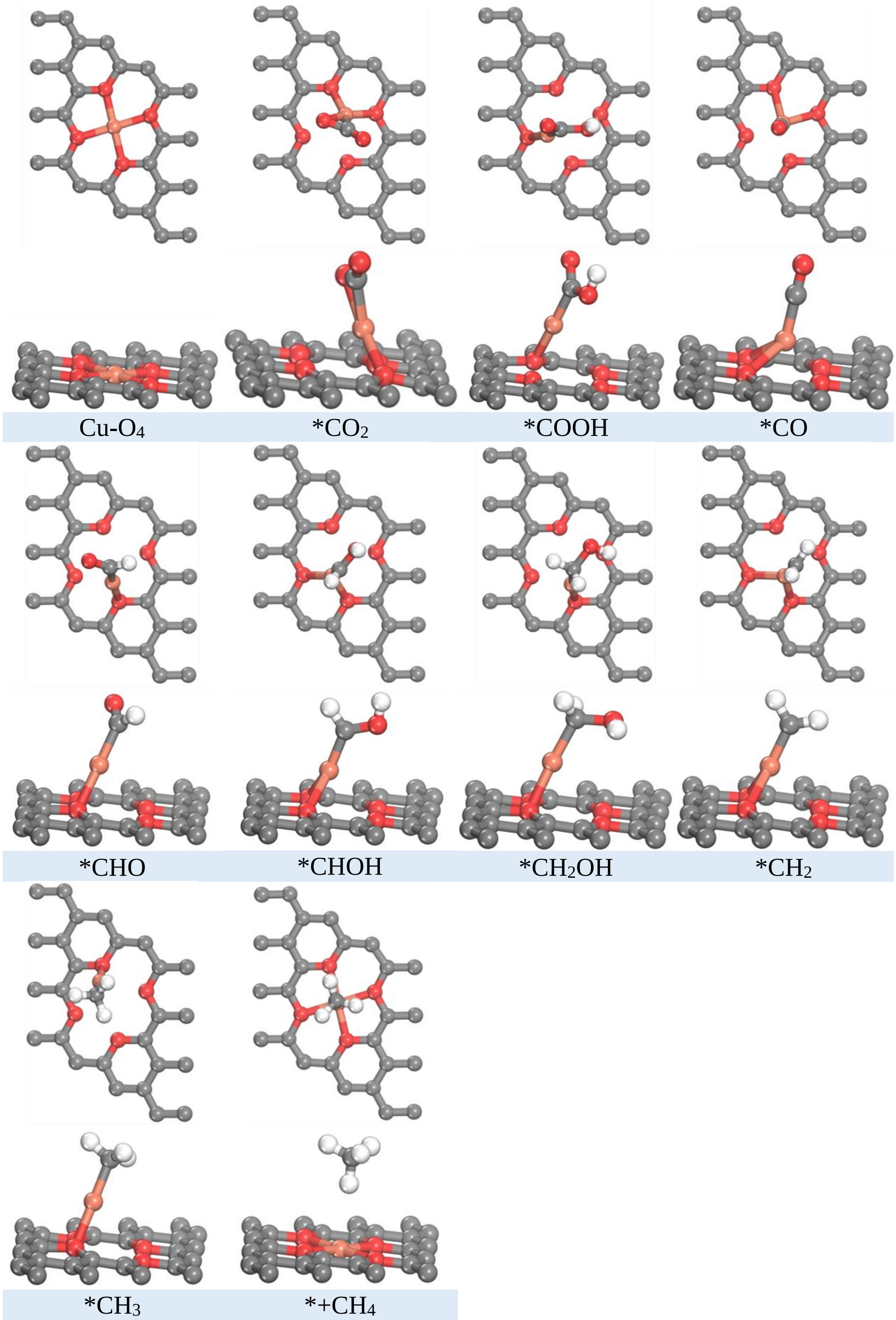

Figure S7. Top and side views of the optimized configurations involved in the reaction pathway for CH_4 formation on Cu-O_4 SAC.

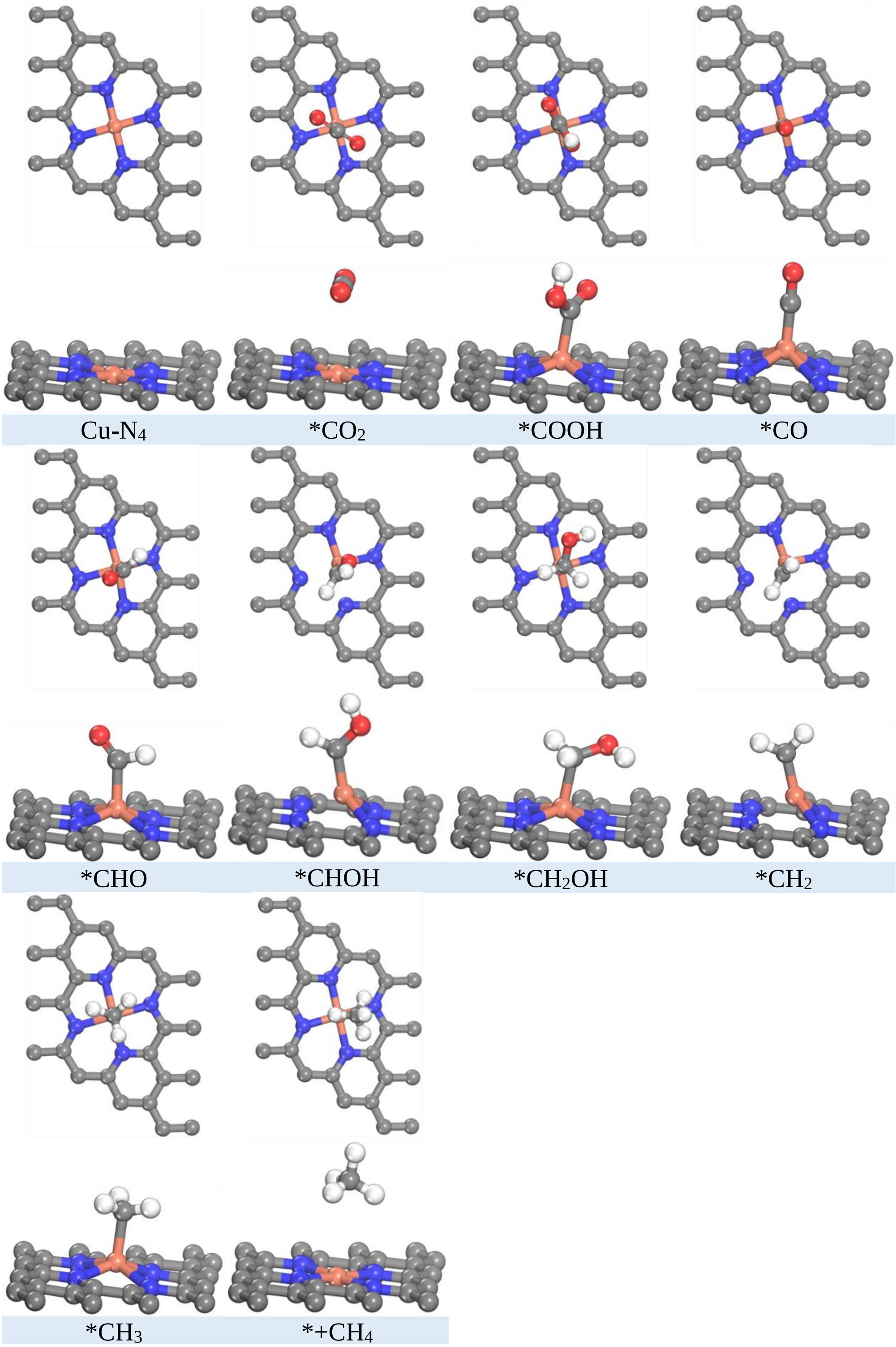

Figure S8. Top and side views of the optimized configurations involved in the reaction pathway for CH_4 formation on Cu-N_4 SAC.

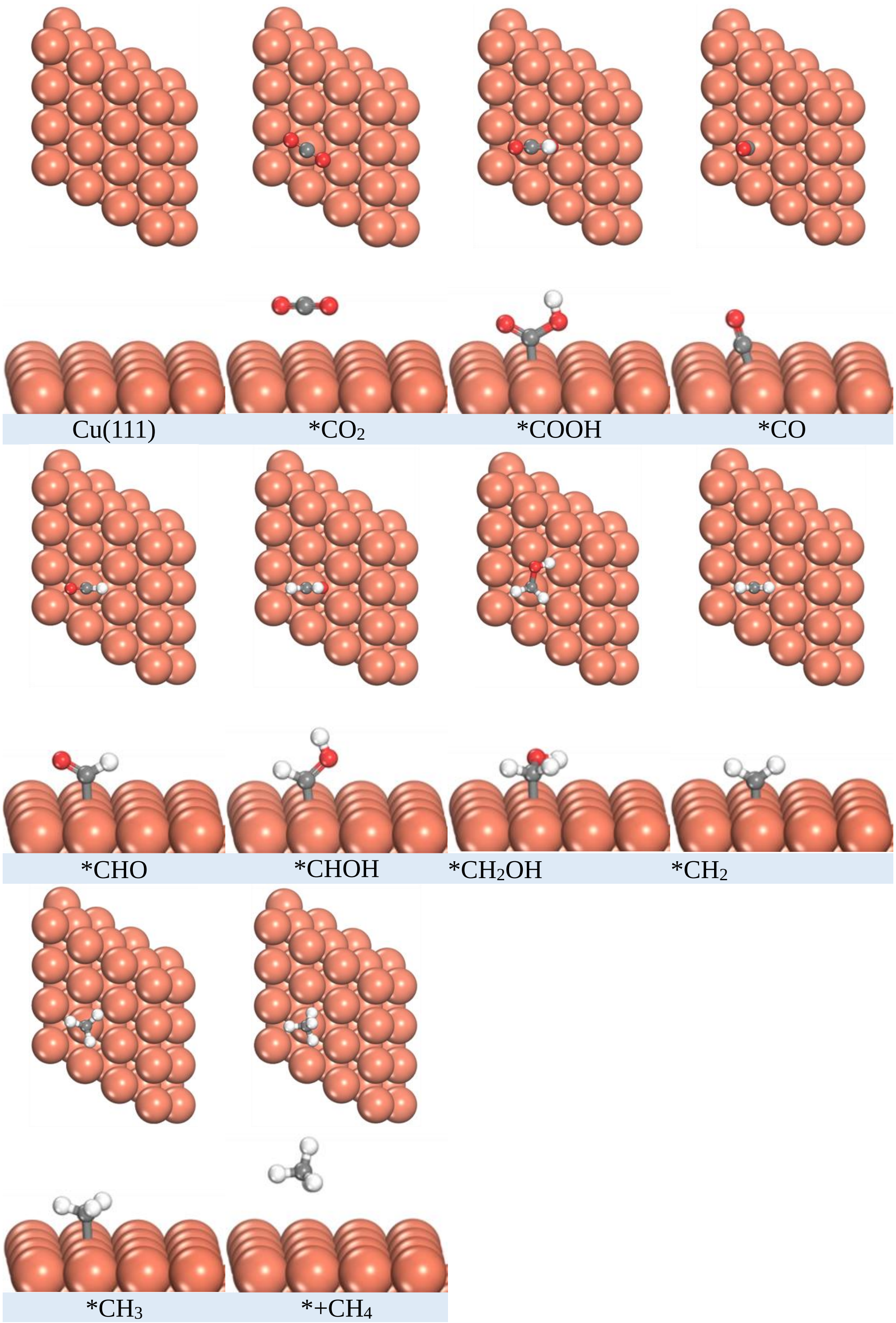

Figure S9. Top and side views of the optimized configurations involved in the reaction pathway for CH_4 formation on Cu (111).

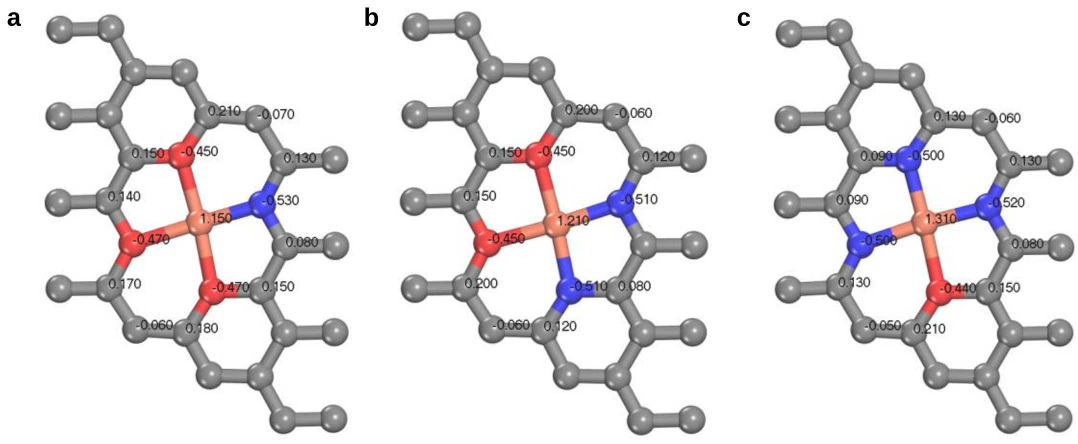

Figure S10. Bader charge of Cu-O_3N SAC, Cu-O_2N_2 SAC, Cu-ON_3 SAC.

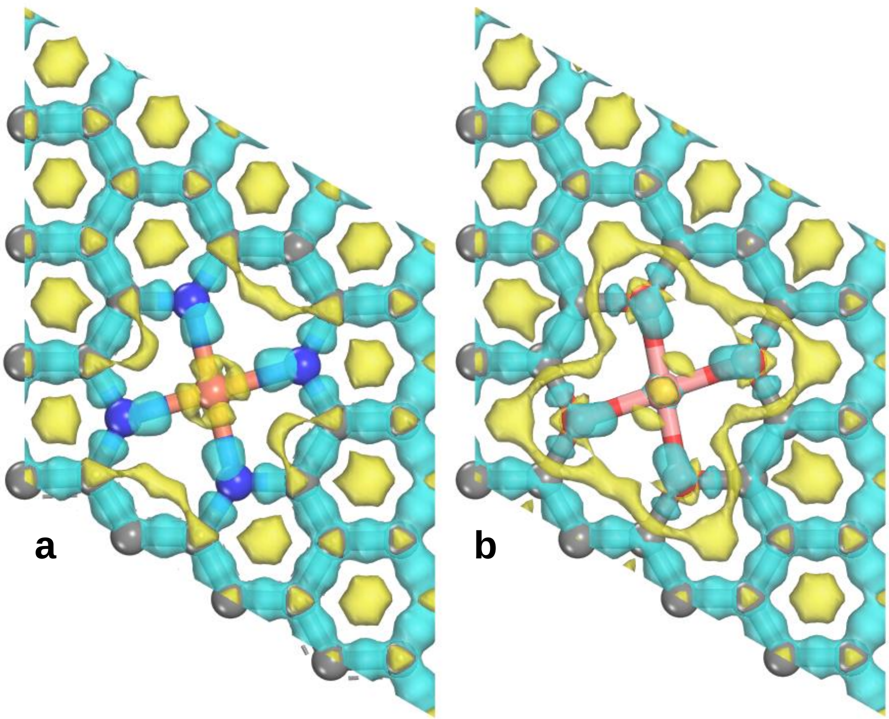

Figure S11. Differential charge density of Cu-O_4 SAC and Cu-N_4 SAC.

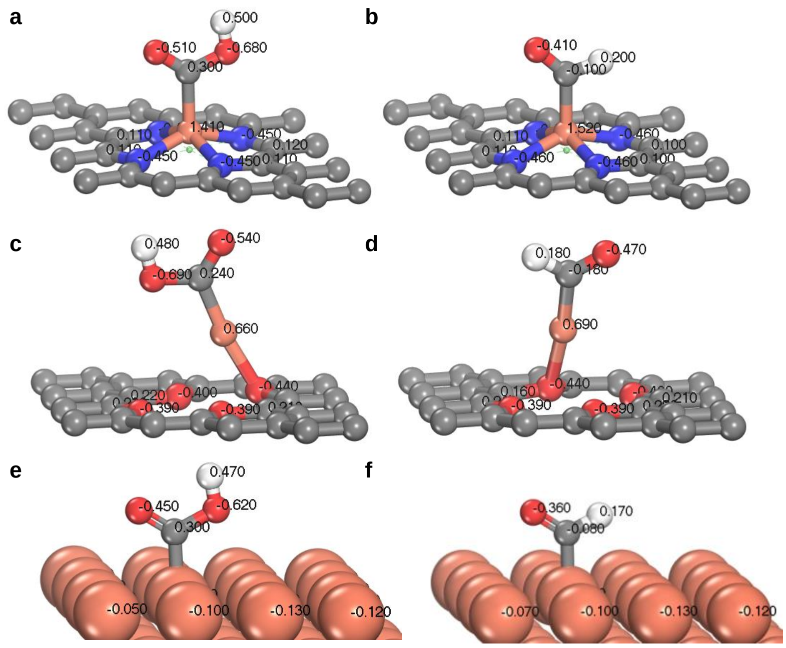

Figure S12. Bader charge of COOH and CHO on (a-b) Cu-N_4 SAC, (c-d) Cu-O_4 SAC and (e-f) Cu (111).

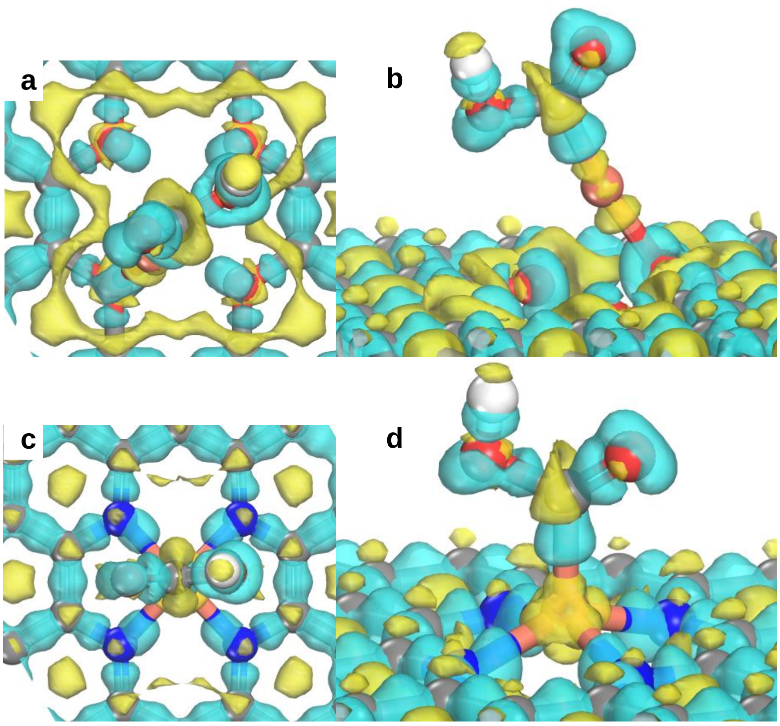

Figure S13. Differential charge density of COOH on Cu-O_4 SAC. (a) top view and (b) side view. Differential charge density of COOH on Cu-N_4 SAC. (c) top view and (d) side view.

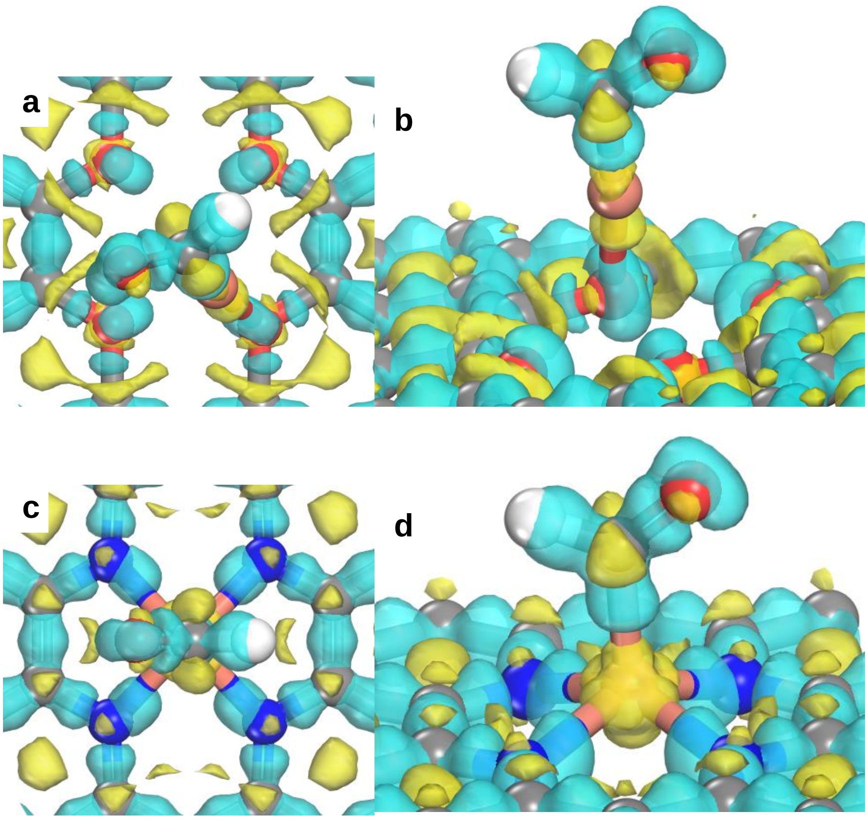

Figure S14. Differential charge density of CHO on Cu-O_4 SAC. (a) top view and (b) side view. Differential charge density of CHO on Cu-N_4 SAC: (c) top view and (d)side view.

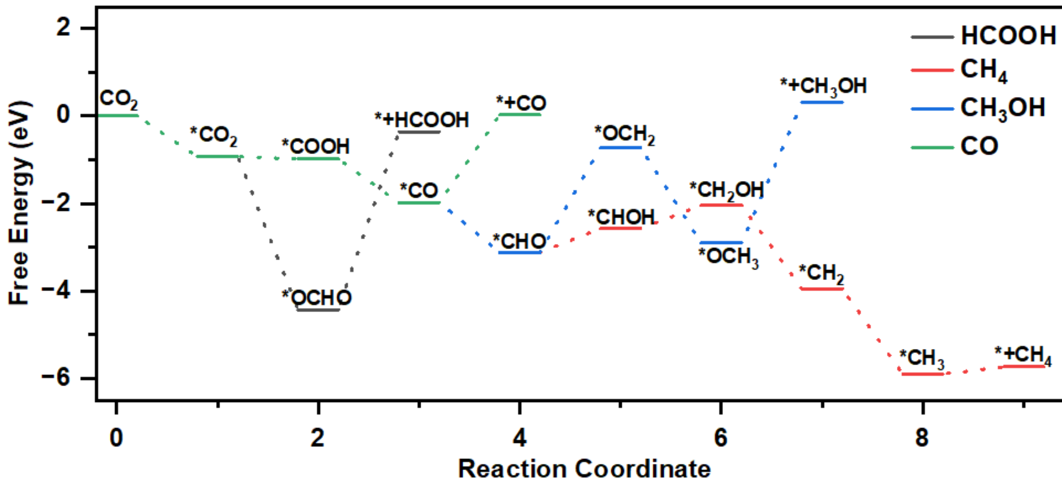

Figure S15. Gibbs free energy diagram of CH_4, CO, HCOOH and CH_3OH by eCO_2RR on Cu-O_4 SAC.

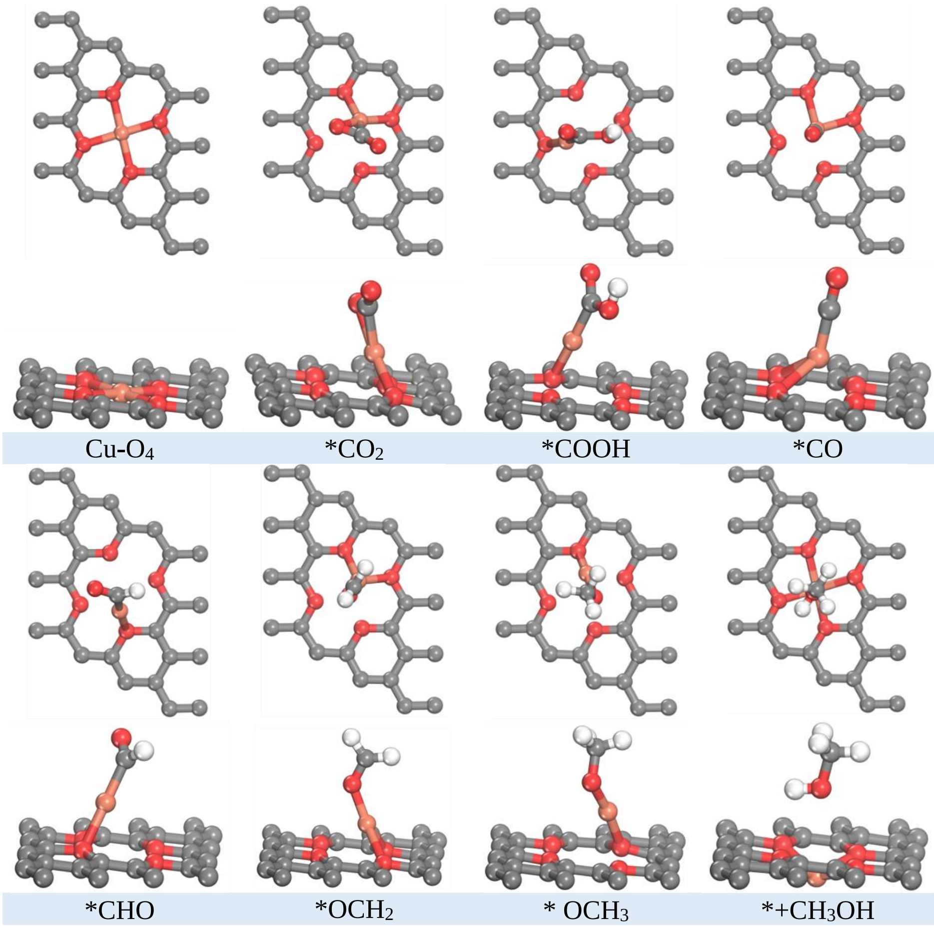

Figure S16. Top and side views of the optimized configurations of adsorbed species involved in the reaction pathway for CH_3OH formation on Cu-O_4 SAC.

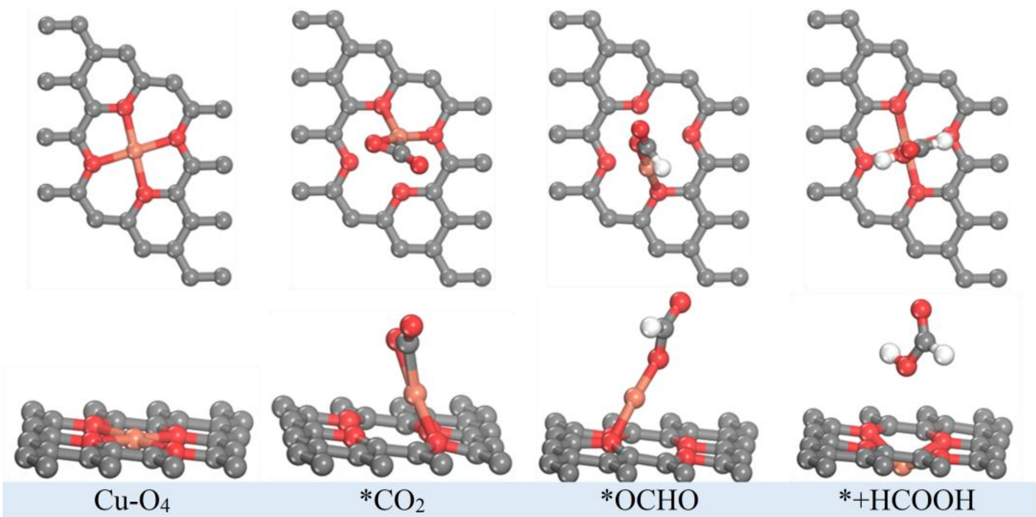

Figure S17. Top and side views of the optimized configurations involved in the reaction pathway for HCOOH formation on Cu-O_4 SAC.

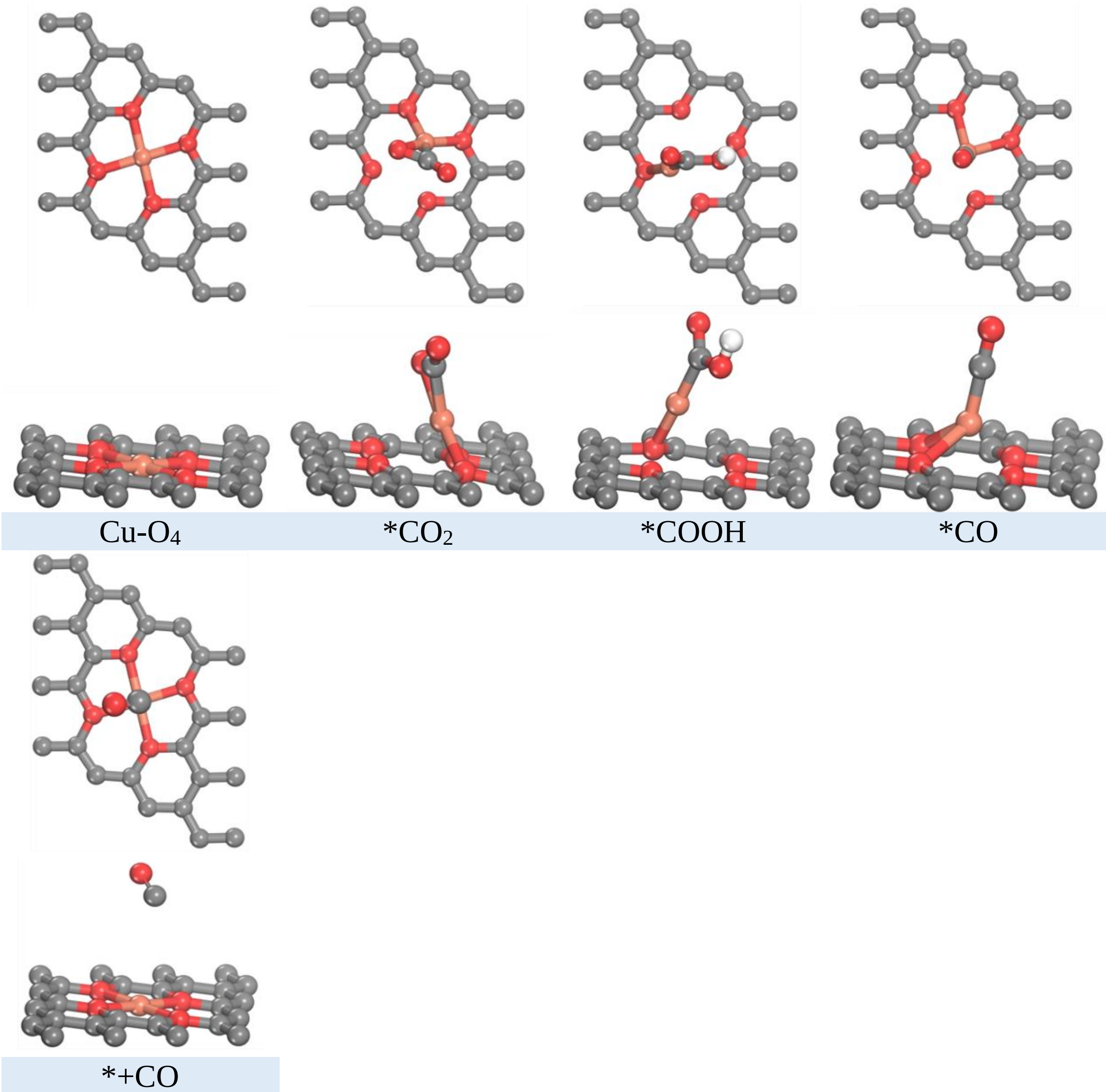

Figure S18. Top and side views of the optimized configurations involved in the reaction pathway for CO formation on Cu-O_4 SAC.

Table S1. Structural parameters of the Cu SAC obtained from EXAFS fitting

Sample	Path	N	R (Å)	ΔE_0(eV)	σ^2×103(Å^2)	R factor
Cu	Cu-O	3.9	1.93	–1.053	4.09	0.019

N, coordination number; R, distance between absorber and backscatter atoms; ΔE_0, inner potential correction to account for the difference in the inner potential between the sample and the reference compound. σ^2, Debye–Waller factor; S_0^2 fitting from Cu sample defined as 0.79.

Table S2. Performance comparison of eCO_2RR to CH_4 of Cu-O_4 SAC with reported catalysts

Catalysts	Electrolyte/ Device	Potential (V vs. RHE)	J_{CH4} ($mA \cdot cm^{-2}$)	FE_{CH4} (%)	TOF (s^{-1})	Ref.
Cu-O_4 SAC	1 M KOH/F-Cell	–1.00	–200.0	63	3.67	This work
CuSiOx	1 M KOH/F-Cell	–1.60	–170.0	60.00		[1]
Cu-TBrPP	1 M KOH/F-Cell	–1.00	–173.6	55.80	0.50	[2]
Cu_4I	1 M KOH/F-Cell	–1.08	–60.7	57.20	NA	[3]
EDTA/CNT	0.5 M $KHCO_3$/H-Cell	–1.30	−16.5	61.6	NA	[4]
CuTAPP	0.5 M $KHCO_3$/F-Cell	–1.63	–142.0	54.80	0.28	[5]
m-Cu NPs	0.1 M $KHCO_3$/H-Cell	–1.30	–10.9	50.00	NA	[6]
Cu/CeO_2-R	0.1 M $KHCO_3$/H-Cell	–1.60	–16.0	49.30	2.22	[7]
Cu-FeSA	1 M $KHCO_3$/F-Cell	–1.10	–128.0	64.00	8.83	[8]
Cu-PorOH	0.5 m $KHCO_3$/H-Cell	–1.50	–23.2	51.30	48.30	[3]
Cu NWs	0.1M $KHCO_3$/H-Cell	–1.25	–7.5	55.00	NA	[9]
La_5Cu_{95}	0.5 M $KHCO_3$/F-Cell	–1.72	–193.5	64.50	NA	[10]
Cu@NC-3	0.1 M $KHCO_3$/H-Cell	–1.65	–30.0	30.00	NA	[11]
Ag-Cu_2O-3	0.1 M $KHCO_3$/H-Cell	–1.50	–13.1	62.00	2.36	[12]
Cu	1 M $KHCO_3$/F-Cell	–1.40	–108.0	48.00	NA	[13]

Table S3. Double layer capacitance and electrochemical active area of Cu/C and Cu SAC

Sample	Cu/C	Cu SAC
C_{dl} (mF/cm^2)	25.6	22
ECSA (cm^2)	0.64	0.24

References

1. Tan X, Sun K, Zhuang Z, Hu B, Zhang Y, et al. Stabilizing Copper by a Reconstruction-Resistant Atomic Cu–O–Si Interface for Electrochemical CO_2 Reduction[J]. *Journal of the American Chemical Society*, **2023**, 145(15): 8656-8664.http://dx.doi.org/10.1021/jacs.3c01638
2. Jiang H, Zhao P, Shen H, Yang S, Gao R, et al. New Insight into the Electronic Effect for Cu Porphyrin Catalysts in Electrocatalytic of CO_2 into CH_4[J]. *Small*, **2024**, 20(2): 2304998.http://dx.doi.org/https://doi.org/10.1002/smll.202304998
3. Zhang Y, Zhou Q, Qiu Z-F, Zhang X-Y, Chen J-Q, et al. Tailoring Coordination Microenvironment of Cu(I) in Metal–Organic Frameworks for Enhancing Electroreduction of CO_2 to CH_4[J]. *Advanced Functional Materials*, **2022**, 32(36): 2203677.http://dx.doi.org/https://doi.org/10.1002/adfm.202203677
4. Huang M X, Gong S P, Wang C L, Yang Y, Jiang P, et al. Lewis-Basic EDTA as a Highly Active Molecular Electrocatalyst for CO_2 Reduction to CH_4[J]. *Angewandte Chemie International Edition*, **2021**, 60(42): 23002-23009.http://dx.doi.org/10.1002/anie.202110594
5. Yu P E, Lv X M, Wang Q H, Huang H L, Weng W J, et al. Promoting Electrocatalytic CO_2 Reduction to CH_4 by Copper Porphyrin with Donor-Acceptor Structures[J]. *Small*, **2023**, 19(4).http://dx.doi.org/10.1002/smll.202205730
6. Kim M K, Kim H J, Lim H, Kwon Y, Jeong H M. Metal-organic framework-mediated strategy for enhanced methane production on copper nanoparticles in electrochemical CO_2 reduction[J]. *Electrochimica Acta*, **2019**, 306: 28-34.http://dx.doi.org/10.1016/j.electacta.2019.03.101

7. Xue L, Zhang C J, Wu J F, Fan Q Y, Liu Y, et al. Unveiling the reaction pathway on Cu/CeO_2 catalyst for electrocatalytic CO_2 reduction to CH_4[J]. *Applied Catalysis B: Environment and Energy*, **2022**, 304.http://dx.doi.org/10.1016/j.apcatb.2021.120951
8. Hung S-F, Xu A, Wang X, Li F, Hsu S-H, et al. A metal-supported single-atom catalytic site enables carbon dioxide hydrogenation[J]. *Nature Communications*, **2022**, 13(1): 819.http://dx.doi.org/10.1038/s41467-022-28456-9
9. Li Y F, Cui F, Ross M B, Kim D, Sun Y, et al. Structure-Sensitive CO_2 Electroreduction to Hydrocarbons on Ultrathin 5-fold Twinned Copper Nanowires[J]. *Nano Letters*, **2017**, 17(2): 1312-1317.http://dx.doi.org/10.1021/acs.nanolett.6b05287
10. Zhao J, Zhang P, Yuan T H, Cheng D F, Zhen S Y, et al. Modulation of *CHXO Adsorption to Facilitate Electrocatalytic Reduction of CO2 to CH4 over Cu-Based Catalysts[J]. *Journal of the American Chemical Society*, **2023**, 145(12): 6622-6627.http://dx.doi.org/10.1021/jacs.2c12006
11. Jiang C J, Hou Y, Liu H, Wang L T, Zhang G R, et al. CO_2 electrocatalytic reduction on Cu nanoparticles loaded on nitrogen- doped carbon[J]. *Journal of Eelectroanalytical Chemistry*, **2022**, 915.http://dx.doi.org/10.1016/j.jelechem.2022.116353
12. Sun M, Zhang L X, Tian F L, Li J X, Lei Y Q, et al. Mechanistic investigation on Ag-Cu_2O in electrocatalytic CO_2 to CH_4 by in situ/operando spectroscopic and theoretical analysis[J]. *Journal of Energy Chemistry*, **2024**, 88: 521-531.http://dx.doi.org/10.1016/j.jechem.2023.10.004
13. Wang X, Xu A N, Li F W, Hung S F, Nam D H, et al. Efficient Methane Electrosynthesis Enabled by Tuning Local CO_2 Availability[J]. *Journal of the American Chemical Society*, **2020**, 142(7): 3525-3531.http://dx.doi.org/10.1021/jacs.9b12445